0026-895X/97/030475-09$3.00/0

MOLECULAR PHARMACOLOGY, **51:**475–483 (1997).

Voltage-Dependent Inhibition of RCK1 K^+ Channels by Phenol, *p*-Cresol, and Benzyl Alcohol

A. A. ELLIOTT and J. R. ELLIOTT

Department of Anatomy and Physiology, University of Dundee, Dundee, Scotland

Received August 6, 1996; Accepted December 3, 1996

SUMMARY

Phenol has various medical applications but can cause convulsions and cardiac arrhythmia suggestive of K^+ channel block. We examined phenol inhibition of the delayed-rectifier RCK1 (Kv1.1) K^+ channel cloned from rat brain and expressed in *Xenopus laevis* oocytes. Phenol (2.5 mM) caused a 43 ± 5 mV depolarizing shift in the RCK1 half-activation voltage (V_g) but only a 10 ± 3% decrease in the peak conductance at 80 mV. The 10–90% rise time was slightly increased, but this was not simply the result of the activation shift. By contrast, deactivation kinetics at −40 mV were greatly accelerated. The importance of the phenolic hydroxyl group was assessed by comparing the effects of *p*-cresol (a phenol) and its structural isomer benzyl alcohol (an aryl alcohol). *p*-Cresol (1.5 mM) produced a 53 ± 2 mV depolarizing shift in V_g, but benzyl alcohol was much less effective—20 mM caused a depolarizing shift of only 23 ± 1 mV. Both isomers also accelerated channel deactivation. Phenol and *p*-cresol are better hydrogen bond donors than acceptors, whereas benzyl alcohol is a better acceptor than donor. A hydrogen bond between the phenolic hydroxyl and a presently unknown acceptor group may therefore underlie some aspects of K^+ channel inhibition. Depolarizing shifts in V_g and accelerated tail kinetics are consistent with 1) preferential phenol binding to resting channels, causing the shift in V_g, and 2) a conducting phenol-bound open state with faster deactivation kinetics than the unbound open state.

Phenol has a number of clinical applications [e.g., the induction of chronic nerve block (1) and chemical face peeling (2)]. Serum phenol levels can be as high as 3.6 mM after chemical peels (3). It has been suggested that clinical phenol administration may lead to cardiac dysrhythmia (1–4), which emphasizes the need to identify phenol-induced changes in ion channel gating. In the laboratory, phenol causes convulsions in mice (5) and has a facilitatory action at the skeletal neuromuscular junction (6). These effects imply significant changes in nerve and muscle excitability, but relatively little is known concerning the actions of phenol on voltage-gated ion channels. Kaila and Saarikoski (7) suggest that phenol and its weakly acidic derivatives produce a fairly specific inhibition of voltage-dependent potassium conductance in crayfish giant axons but did not demonstrate this action under voltage clamp. Zamponi and French (8) reported a much greater block by phenol of cardiac sodium channels compared with those from skeletal muscle. However, these were batrachotoxin-activated channels in planar bilayers, and such channels do not gate normally.

Our first aim was to determine the effects of phenol on rat brain RCK1 (Kv1.1) potassium channels expressed in *Xenopus laevis* oocytes. When injected without additional β-subunits, these channels act as delayed rectifiers (9). Phenols and alcohols both contain a hydroxyl group; in phenols, the hydroxyl oxygen is attached directly to the benzene ring, whereas in aryl alcohols, one or more intermediate methylene groups separate the two. This has a major effect on the acidity of the hydroxyl hydrogen and on the hydrogen bond donor versus acceptor character of the molecule (10). Our second aim was to compare the effects of two methods of adding a methylene group to the phenol molecule (Fig. 1). Addition at the 4 position of the benzene ring gives *p*-cresol, a phenol. Insertion between the ring and the hydroxyl group gives benzyl alcohol, an aryl alcohol. This comparison confirmed the importance of the phenol hydroxyl group and, presumably, the phenolic hydrogen bond, because *p*-cresol was found to be slightly more potent, and benzyl alcohol much less potent, than phenol. A preliminary account of some of this work has been presented to the Physiological Society (11).

Materials and Methods

cRNA preparation and injection. Cloned cDNA (a gift from Prof. O. Pongs, Hamburg, Germany) was transcribed *in vitro* using the mMessage mMachine kit from Ambion (Austin, TX). Stage V–VI

This work was supported by the Wellcome Trust and the University of Dundee.

ABBREVIATIONS: HEPES, 4-(2-hydroxyethyl)-1-piperazineethanesulfonic acid; V_g, half-activation voltage; ΔV_g, shift in V_g; k_g, mid-point slope of the activation curve; g_K, chord conductance; I-V, current-voltage.

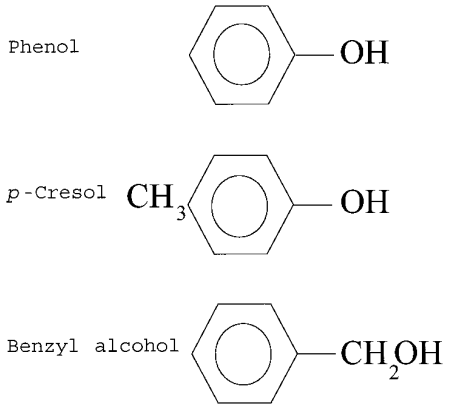

Fig. 1. Structures of phenol, *p*-cresol, and benzyl alcohol.

oocytes were isolated from the ovarian lobes of *X. laevis* frogs and defolliculated by incubation for 1–3 hr at room temperature in a solution of 0.03% collagenase (Type XI; Sigma, Poole, UK) in calcium-free OR2 solution (80 mM NaCl, 2 mM KCl, 1 mM $MgCl_2$, 2.5 mM Na-HEPES, 2.5 mM HEPES, pH 7.5, with NaOH). The frogs were anesthetized in a solution of 0.15–0.35% tricaine in ice water and either killed by destruction of the brain or allowed to recover after the surgery for one further operation. Oocytes were injected with 50 nl of capped RNA (0.1–0.5 $\mu g/\mu l$) using a Nanoliter Injector (World Precision Instruments, Stevenage, Hertfordshire, UK) and were incubated in modified Barth's medium [78 mM NaCl, 1 mM KCl, 2.4 mM $NaHCO_3$, 0.82 mM $MgSO_4$, 0.33 mM $Ca(NO_3)_2$, 0.41 mM $CaCl_2$, 10 mM Na-HEPES, 10 mM HEPES, pH 7.2, with NaOH] containing 10 units/ml penicillin and 10 μg/ml streptomycin at 19° for 1–10 days before recording.

Electrophysiological measurements. Whole-cell currents were recorded using a two-microelectrode voltage clamp amplifier specifically designed for recording fast, large-amplitude, voltage-gated currents from oocytes (TURBO TEC 10CD; NPI Electronic, Tamm, Germany). Voltage command pulses were generated, and currents were recorded using a TL-1 interface and pCLAMP 6 software (Axon Instruments, Foster City, CA). All currents were corrected for capacitative and linear leakage currents before analysis using a standard P/4 subtraction protocol. Currents were filtered at 1 kHz, and the sampling frequency was between 3 and 4 kHz. Data were analyzed using Clampfit (Axon Instruments, Foster City, CA), PSI-Plot (Poly Software International, Salt Lake City, UT) and Microsoft Excel (Redmond, WA) software.

The recording electrodes were filled with 2 M KCl (pH 7.2 with 5 mM HEPES and KOH) and had a resistance of between 0.6 and 0.9 MΩ. $Ag/AgCl_2$ pellets were used as reference electrodes. The bath solution was normal frog Ringers solution (110 mM NaCl, 2.5 mM KCl, 1.8 mM $CaCl_2$, 5 mM Na-HEPES, 5 mM HEPES, pH 7.2, with NaOH), and solutions were exchanged by total replacement of the bath medium. All experiments included control, test, and wash. The chemicals used were Analar grade from BDH Chemicals or Sigma (both Poole, Dorset, UK). The phenol was 99.5% pure and the benzyl alcohol 99% pure (Sigma); the *p*-cresol was 99% pure (Aldrich Chemical, Gillingham, Dorset, UK).

Experiments were performed at room temperature (23 ± 2°). All numerical data are quoted as mean ± standard error for a minimum of three experiments unless otherwise stated.

Pulse protocols and data analysis. Oocytes were voltage-clamped at a holding potential of −80 mV. The I-V relationship was determined by applying a 200-msec test pulse to between −70 and 80 mV. In many cases, this was immediately followed by a second 200-msec test pulse to −40 mV (tail-IV). The stimulating frequency was 0.2 Hz for an ordinary I-V protocol and 0.1 Hz for a tail-IV. The peak chord conductance (g_K) at each potential was calculated from the corresponding peak current, assuming a reversal potential (V_K) of −80 mV: $g_K = I_K/(V-V_K)$.

The potential at which g_K is half its maximal value (g_{max}) is termed V_g, and the slope factor of the normalized conductance-voltage relationship is termed k_g. V_g and k_g were determined from a least-squares fit of a simple Boltzmann relationship to the data: $g/g_{max} = 1/(1 + \exp((V_g-V)/k_g))$, where g/g_{max} is the normalized g_K and V is the test potential.

Tail currents were fit using single or double exponential functions: amplitude = $A*\exp(-\text{time}/\tau) + C$ and amplitude = $A_{slow}*\exp(-\text{time}/\tau_{slow}) + A_{fast}*\exp(-\text{time}/\tau_{fast}) + C$, where the amplitude at time 0 is $A + C$ or $A_{slow} + A_{fast} + C$, respectively, and C is the amplitude at infinite time. The relative contribution of τ_{fast} was calculated as $A_{fast}/(A_{fast} + A_{slow})$. Fits were started 5 msec after the beginning of the tail voltage step and extrapolated back to the beginning. This time was chosen to avoid a clear settling phase of some 3 msec. All functions were fit to data using the nonlinear regression features of either pCLAMP or PSI-Plot. Ten- to ninety-percent rise times were calculated using pCLAMP.

Numerical models. Numerical simulations of the Hodgkin-Huxley axon and K^+ channel models were made using a fourth order Runge-Kutta algorithm written in QuickBasic (Microsoft, Redmond, WA) and based on that given by Constantinides (12). The integration step size was manually adjusted to give a stable solution.

Results

Phenol. Phenol produced a large but extremely voltage-dependent inhibition of the RCK1 current. Fig. 2A shows the effects of 2.5 mM phenol on currents elicited by test pulses to voltages between −70 and 80 mV, with a subsequent step to −40 mV. The I-V relationship in Fig. 2B shows almost total suppression at low depolarizations and near zero suppression at high depolarizations. Onset and offset of all drug effects immediately followed commencement of solution changes. Averaged data for fractional block by 1, 2.5, 4, and 8 mM phenol are shown in Fig. 2C. Even 1 mM caused more than 85% inhibition at −40 mV. The voltage-dependent nature of the inhibition makes the quotation of a single IC_{50} value somewhat arbitrary. One possibility is to consider the degree of block at the voltage that causes 50% activation of control channels, which is close to −30 mV. One millimolar phenol caused 78 ± 1% block at −30 mV (Table 1); therefore, the IC_{50} on this scale is somewhat less than 1 mM.

The voltage-dependent block by phenol is linked to a depolarizing shift in the activation curve. Averaged data for the effects of 1 and 2.5 mM phenol on the voltage dependence of channel activation are given in Fig. 2, D and E. Even 1 mM phenol caused a 13-mV depolarizing shift in V_g, the potential for 50% activation, and 2.5 mM gave a massive shift of more than 40 mV.

The fall in control RCK1 conductance at high potentials and the plateauing of the I-V relationship result from a voltage-dependent block by internal magnesium (13). This phenomenon does not affect the main conclusions regarding the effects of phenol and the other compounds studied. It would, however, complicate the comparison of peak conductances in control and test conditions, as the phenol-treated currents reach full activation at more depolarized voltages than the control currents (i.e., at potentials in which there is greater magnesium block). We have therefore compared con-

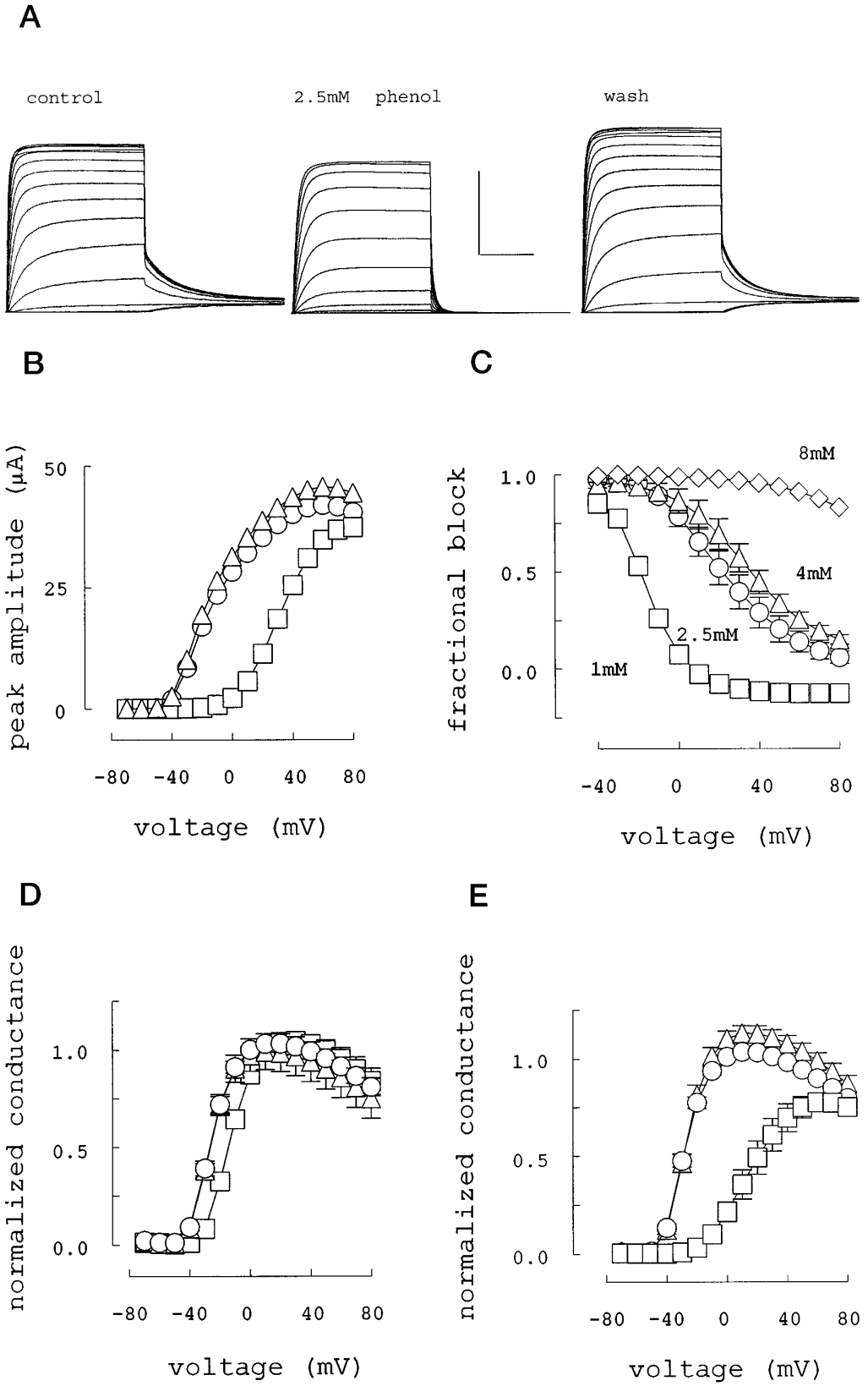

Fig. 2. Voltage-dependent RCK1 current inhibition by phenol. Experimental currents (A) and an I-V relationship (B) demonstrate the effect of 2.5 mM phenol. *Scale bars,* 20 μA and 100 msec. C, Averaged data show the reduction in peak current caused by 1, 2.5, 4, and 8 mM phenol. The fractional block was calculated as 1 − [2 × test amplitude/(control amplitude + wash amplitude)]. D and E, Depolarizing shifts in the conductance-voltage curve caused by 1 and 2.5 mM phenol, respectively. Test and wash data from each individual experiment were normalized with respect to the maximal control conductance for that oocyte before constructing the mean curves shown herein. Phenol caused substantial depolarizing shifts in activation voltage dependence with relatively little effect on the conductance at 80 mV. ○, control; □, test; △, wash.

ductances at a constant potential of 80 mV, where 2.5 mM phenol is seen to cause only a 10% fall (Table 1).

Fig. 3 shows the effects of 2.5 mM phenol on channel kinetics. Phenol slows the current rising phase (Fig. 3, A and C) and greatly accelerates the speed of closure at −40 mV (Figs. 2A and 3B). However, the increase in rise time induced by 2.5 mM phenol is much less than that which would result directly from a 43-mV depolarizing shift of the control curve along the

TABLE 1

Summarized effects of phenol, *p*-cresol and benzyl alcohol on the RCK1 channel

One hundred percent block indicates total suppression of the current. ↓ and ↑ indicate decrease and increase respectively. A change from 4 to 8 is a 100% increase, a change from 8 to 4 is a 50% decrease. The potential is shown where appropriate. g_k is the peak chord conductance, ΔV_g the change in potential for 50% activation and k_g the slope of the normalized conductance-voltage curve. τ_{fast} and τ_{slow} are the time constants derived from double exponential fits to tail currents. Drug treatment not only reduces both time constants but also increases the contribution of τ_{fast}. All experiments had a wash phase and effects are calculated as test relative to the mean of control and wash.

Compound and conc^n	% block at −30 mV	% ↓ in g_k at 80 mV	ΔV_g (mV)	% ↑ in k_g	% ↑ in rise time at 80 mV	% ↓ in deactivation τ_{fast} (80 to −40 mV)	% ↑ in deactivation τ_{slow} (80 to −40 mV)	% ↑ contribution of deactivation τ_{fast} (80 to −40 mV)
1.0 mM phenol	78 ± 1	−8 ± 3	13 ± 0	14 ± 1	18 ± 2	NA	NA	NA
2.5 mM phenol	98 ± 0	10 ± 3	43 ± 5	58 ± 5	95 ± 15	65 ± 8	61 ± 2	232 ± 44
1.5 mM *p*-cresol	98 ± 0	12 ± 1	53 ± 2	64 ± 8	235 ± 28	55 ± 7	56 ± 3	109 ± 27
8 mM benzyl alcohol	65 ± 2	3 ± 2	9 ± 0	7 ± 1	1 ± 2	23 ± 8	25 ± 3	113 ± 20
20 mM benzyl alcohol	95 ± 0	25 ± 0	23 ± 1	34 ± 3	1 ± 2	66 ± 4	59 ± 2	120 ± 20

voltage axis (Fig. 3C). This departure from a simple shift along the voltage axis was also evident with 4 and 8 mM phenol. The tail current decay could be adequately fit by a first-order exponential function (the visibly separate lines in Fig. 3B are first-order fits), but a second-order function gave a near perfect fit (the second-order fits in Fig. 3B are indistinguishable from the data). Analysis of 16 control experiments gave a τ_{fast} of 17 ± 1 msec, a τ_{slow} of 52 ± 2 msec, and a 30 ± 3% contribution of the fast process to the control decay. Phenol (2.5 mM) reduced both the fast and slow time constants (by 65 ± 8% and 61 ± 2%, respectively) and increased the relative contribution of τ_{fast} to 84 ± 2%; i.e., it more than doubled the contribution of the fast decay.

Benzyl alcohol and *p*-cresol. The effects of 20 mM benzyl alcohol on RCK1 currents are compared with those of 1.5 mM *p*-cresol in Fig. 4. *p*-Cresol was more potent than phenol, but even 20 mM benzyl alcohol had less effect on V_g than did 2.5 mM phenol. Benzyl alcohol caused more high-depolarization block than either phenol or *p*-cresol (Fig. 4C). Both *p*-cresol and benzyl alcohol accelerated tail kinetics (Fig. 4, A and B), but benzyl alcohol had little effect on the 10–90% rise time (Fig. 4D), whereas *p*-cresol produced the largest slowing of activation kinetics (Fig. 4E). Both compounds caused depolarizing shifts in the voltage dependence of activation (Fig. 4, D and E).

Discussion

Phenol and the firing behavior of excitable cells. Phenol has a biphasic effect on the excitability of isolated preparations and whole organisms. At relatively high concentrations (7–10 mM), phenol blocks nervous conduction (14, 15). By contrast, 0.25 mM phenol increases the frog end-plate potential (6), and low doses facilitate neuromuscular transmission in the cat (16) and produce convulsions in mice (5). We have shown that phenol produces a voltage-dependent inhibition of RCK1 channels and that this inhibition is associated with substantial depolarizing shifts in the activation threshold. Concentrations in the range known to exist in phenol-treated patients [up to 3.6 mM (3)] induce depolarizing shifts of 13 mV (1 mM) and 43 mV (2.5 mM) in the RCK1 conductance-voltage relationship. Such shifts, even without K^+ channel block at high potentials, are effective in producing spontaneous firing in a model axon, and that firing continues when most of the Na^+ channels are also blocked. Fig. 5 compares the effect on the firing behavior of the Hodgkin-Huxley model squid axon of a 15-mV shift in the K^+ channel activation voltage dependence with that of a 50% voltage-independent K^+ channel block. There is no electrical stimulation; therefore, the control axon does not fire (data not shown). When a 15-mV bias voltage is added to the K^+ channel activation parameter (n), the axon fires spontaneously at 75 Hz. Voltage-independent block of 50% of the K^+ channels also causes spontaneous firing, but at only 50 Hz. The phenol-treated axon continues to fire spontaneously even when 80% of the Na^+ channels are blocked. A 90% Na^+ channel block is required to damp the phenol-induced spontaneous firing. By contrast, when the K^+ channel block is voltage-independent, a 30% Na^+ channel block damps firing. Phenol (10 mM) causes 50–60% block of rat brain IIa Na^+ channels in *X. laevis* oocytes (17). The biphasic effect of phenol on excitability is thus consistent with the combination of a substantial influence on K^+ channel gating and a less potent inhibition of Na^+ channels.

Mechanisms and drug-site interactions. Our aims in the next two sections are to discuss possible mechanisms of action while recognizing that benzyl alcohol is a less, and *p*-cresol a slightly more, potent inhibitor of RCK1 channel than phenol.

Reyes and Latorre (18) found that 19 mM benzyl alcohol reduces the surface dipole potential of bacterial phosphatidylethanolamine monolayers by 20 mV, whereas 51 mM caused a 60-mV reduction. Our observation of a 23-mV shift in the voltage dependence of RCK1 channel activation for 20 mM benzyl alcohol is thus in the same range as the change in phosphatidylethanolamine monolayer surface potential. However, for that effect to be fully translated into a gating shift, one would require either an extremely asymmetrical adsorption of benzyl alcohol [such that the reduction in dipole potential took place only at the inner surface of the membrane (19)] or that the peak of the energy barrier for the voltage-dependent activation transition be located almost entirely within one membrane dipole layer (20). Furthermore, a simple surface potential effect would induce a uniform shift in all gating parameters; i.e., the changes in rise times, for example, would be accounted for by a shift in the control curve. We did not find this to be the case in our study.

Phloretin is a phenolic compound with a dipole moment of 5.6 Debye (21). Phloretin also causes large (30 to 40 mV) depolarizing shifts in the voltage dependence of axonal K^+ channel activation (20, 22). Strichartz *et al*. (20) suggest that these shifts are caused by phloretin-induced changes in the axonal membrane surface dipole potential. Thus, large shifts

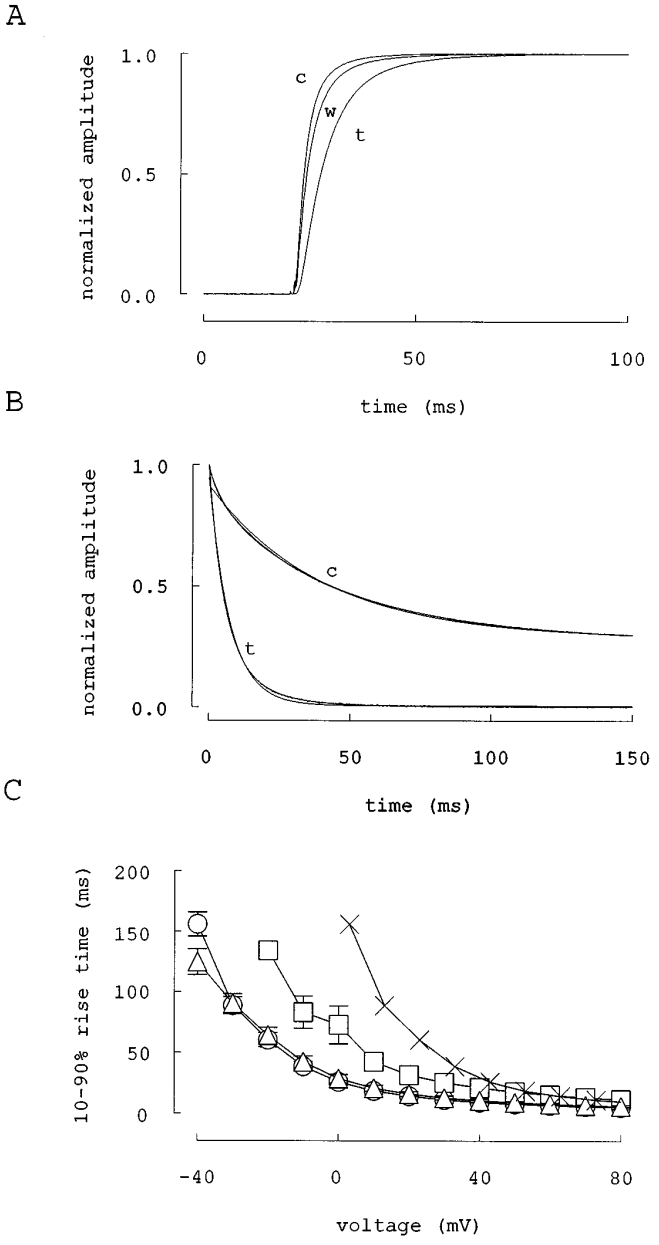

Fig. 3. Phenol slows the RCK1 current rising phase but accelerates channel closure. A, The rising phase of control (*c*), test (*t*), and wash (*w*) current traces at 50 mV from a single experiment with 2.5 mM phenol. B, Tail currents for the control (*c*) and test (*t*) traces. Currents were normalized with respect to the control to facilitate comparison of the rise time and the decay on repolarization to −40 mV. Single and double exponential fits are superimposed on the current tails. Fits are shown extrapolated back to the beginning of the tail voltage step, but the first 5 msec were not included in the fitting process. The single exponential fit is a reasonable approximation but can be distinguished from the data; the double fit is a near perfect match. C, Averaged data show the effects of 2.5 mM phenol on the 10–90% rise time over the full voltage range. The control curve is also shown moved along the voltage axis by an amount equal to the mean shift in half-activation voltage (ΔV_g). Phenol increases the rise time but by an amount much less than that predicted by a simple shift. ○, control; □, test; △, wash; ×, control shifted by ΔV_g mV.

are linked to a large dipole moment, and it seems logical to consider a similar explanation for the effect of phenol on RCK1 channels. However, phenol has a dipole moment of only 1.2 D, whereas benzyl alcohol has a dipole moment of 1.7 D (23). This would not account for the greater effectiveness of phenol without some additional factor that substantially increased phenol adsorption.

Kitagawa and Hirata (24) and Kitagawa *et al.* (25) report the effects of benzyl alcohol, phenol, and *p*-cresol on the membrane fluidity of bovine platelets (determined from changes in the fluorescence anisotropy of diphenylhexatriene) and on platelet aggregation. Twenty millimolar benzyl alcohol, 10 mM phenol, and 5 mM *p*-cresol all caused a 6% reduction in diphenylhexatriene fluorescence anisotropy (indicating an increase in bilayer fluidity) and a 92–98% fall in platelet aggregation. Phenol (1.9 mM) and 1.4 mM *p*-cresol gave a 50% inhibition of aggregation, but the IC_{50} for benzyl alcohol was not reported. It is possible that alterations in channel behavior secondary to membrane fluidity changes account for some of the effects we saw, but the variation in potency for fluidity changes, a factor of 4 between benzyl alcohol and *p*-cresol, is not substantial when compared with the factor of approximately 30 that was found for RCK1 channel gating.

The water-soluble enzyme firefly luciferase is a popular model for the interaction of more or less hydrophobic compounds with purely protein sites of action. Abraham *et al.* (26) give IC_{50} values for phenol and benzyl alcohol of 1.1 and 1.7 mM, respectively. Thus, although the luciferase model has roughly the correct phenol potency, it does not show the required degree of selectivity between phenol and benzyl alcohol.

We suggest that an interaction more specific than fluidity or dipole potential effects is at least partly responsible for K^+ current inhibition by phenol. The comparison of RCK1 channel perturbation by phenol, *p*-cresol, and benzyl alcohol identifies a possible feature of that interaction. Abraham *et al.* (10) describe the partitioning of organic solutes between water and model phases, such as octanol or hexadecane, in terms of six solute properties. Table 2 gives these data for phenol, *p*-cresol, and benzyl alcohol. The striking difference is that both phenol and *p*-cresol are better hydrogen bond donors than acceptors, whereas benzyl alcohol is a better acceptor than donor. This suggests that the partition between phenol and its site of action on, in, or around RCK1 channels involves a strong hydrogen bond in which the phenol hydroxyl group is the donor and some presently unidentified group is the acceptor.

Urban and Haydon (27) propose that the relatively high selectivity of certain halogenated ethers for the squid giant axon delayed rectifier K^+ current over the axonal Na^+ current may also result from channel-specific hydrogen bonds in which acidic hydrogens on the halogenated ether are the donor groups. By contrast, benzyl alcohol, with its weaker donor ability, is much more effective in reducing the squid axon Na^+ current than the K^+ current (28). Rat brain IIa Na^+ channels expressed in *X. laevis* oocytes require 10 mM phenol or 5 mM *p*-cresol for 50–60% inhibition, and those effects are accompanied by a negligible (<3 mV) shift in the voltage dependence of channel activation (17). This supports the suggestion of a specific interaction between phenols and K^+ channels.

Modeling phenol inhibition of RCK1 currents. We now present a simple (but not necessarily unique) model of drug action that reproduces the two most consistent features of phenol, *p*-cresol, and benzyl alcohol perturbation of RCK1

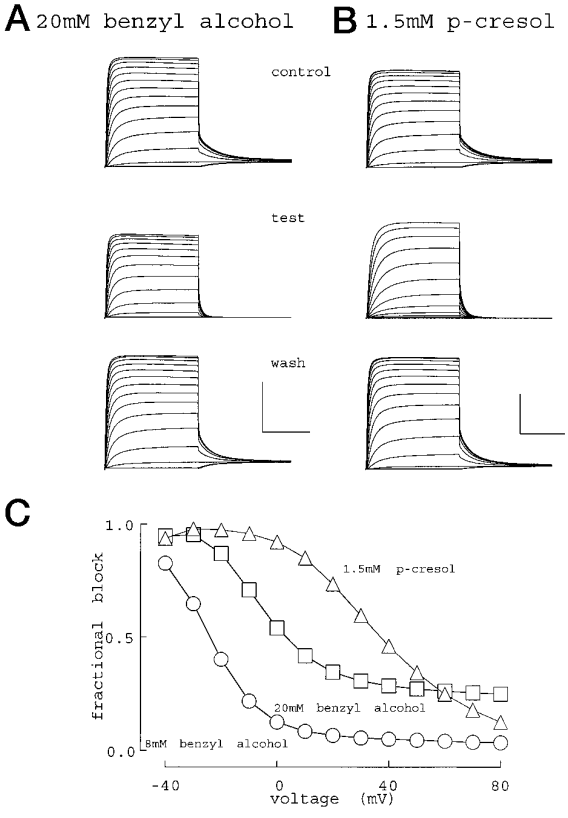

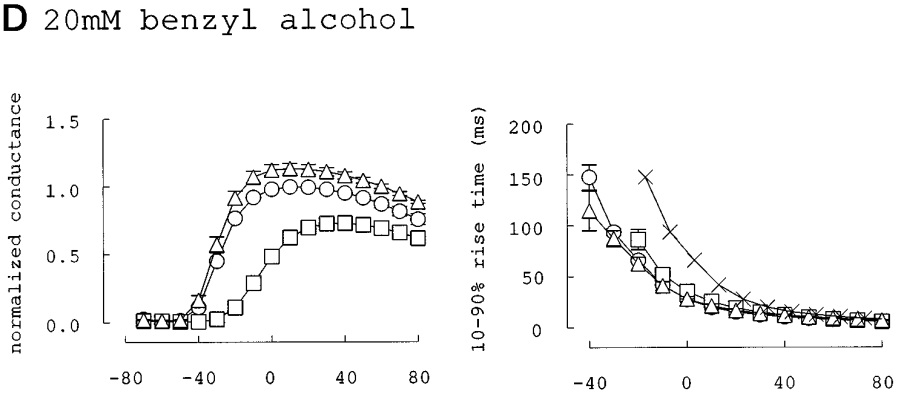

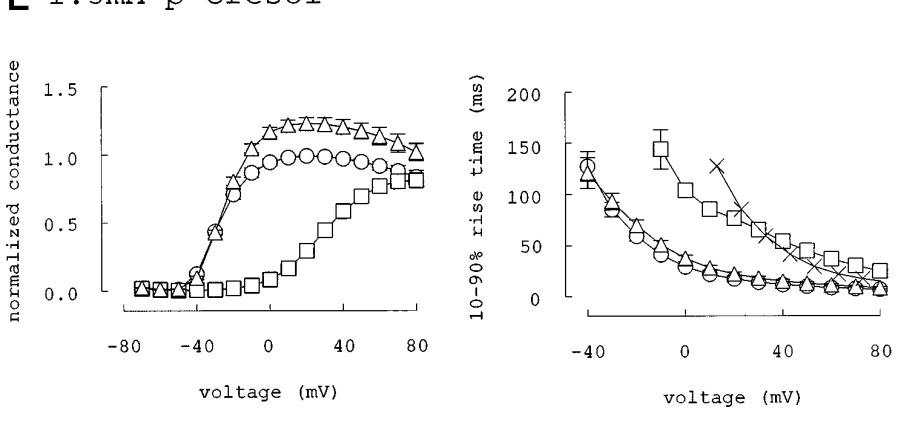

Fig. 4. Effects of benzyl alcohol and *p*-cresol on RCK1 currents. A and B, Currents from single experiments show the effects of 20 mM benzyl alcohol and 1.5 mM *p*-cresol, respectively. Note that although both cause a substantial acceleration of the tail currents at −40 mV, only *p*-cresol noticeably slows the activation kinetics. *Scale bars,* 40 μA and 100 msec (A) and 20 μA and 100 msec (B). C, Voltage dependence of block by 8 and 20 mM benzyl alcohol and 1.5 mM *p*-cresol. Twenty millimolar benzyl alcohol causes a greater high-depolarization block than either *p*-cresol or phenol (see Fig. 2C). D and E, Averaged data show shifts in activation voltage dependence and effect (or lack of effect) on the 10–90% rise time. ×, control rise time data translated by ΔV_g mV. ○, control; □, test; △, wash.

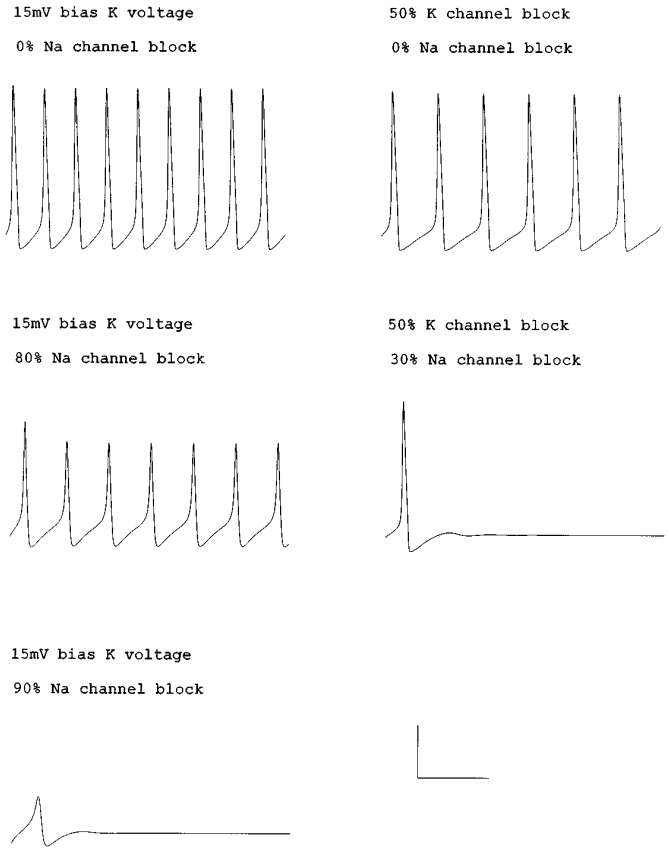

Fig. 5. A depolarizing shift in the voltage dependence of the K^+ channel activation parameter (n) causes spontaneous firing of the Hodgkin-Huxley axon. One hundred-twenty–millisecond duration plots of voltage against time are shown for the electrically unstimulated Hodgkin-Huxley axon. A 15-mV depolarizing shift in the voltage dependence of n (15 mV K bias V) causes spontaneous firing that persists even when 80% of the Na^+ channels are blocked. By contrast, the lower frequency firing induced by a 50% voltage-independent K^+ channel block is critically damped by a loss of only 30% of the Na^+ channels. *Scale bars,* 20 mV and 30 msec.

channels. These are a depolarizing shift in the voltage dependence of channel activation and an acceleration of channel closure on repolarizing to −40 mV. The model and comparisons between simulated and experimental data are shown in Fig. 6. The control channel has four resting states (shown as one group for convenience), a preopen state, and an open state (see, e.g., 29). Drug binding can have two possible effects. One is to simply block the channel, as indicated by the bound blocked state. This accounts for a high-depolarization block but would not cause the depolarizing activation shift or the accelerated tail kinetics. These are produced by including a set of drug-bound resting, preopen, and open states in which the bound open state conducts but is destabilized. In the example given, drug binding destabilizes the open state by causing a 1000-fold increase in β_p, the rate constant to the preopen state. To maintain microscopic reversibility (30), this change in β_p must be matched by making the affinity of the resting and preopen states for the drug 1000 times greater than that of the open state. This was done by reducing the unbinding rate constants (0.003 compared with 3). The rate constants among the various resting states and between the preopen and last resting state were not affected by the drug in this simulation.

Fig. 6B compares simulated currents with averaged control and test data from experiments with 2.5 mM phenol. Fig. 6C shows the match between simulation and experiment for channel activation, and Fig. 6D compares deactivation kinetics. The model does not exactly reproduce the effects of phenol, *p*-cresol, or benzyl alcohol, but that is not surprising given its simple nature. For example, the simulated current tails are all well fit by single exponential functions, and the changes in rise time do not exactly match the experimental findings. However, it does reproduce the depolarizing shift and the reduction in the slope of the activation voltage dependence, and the deactivation kinetics are accelerated. The inclusion of a conducting bound open state was critical to the production of the faster tails.

A 1000-fold decrease in open-state stability is associated with a free energy change of 17 kJ/mol. That is equivalent to roughly twice the combined energy of a hydrogen bond (31) and the interaction between a cation and the benzene ring π electrons (32). It is possible that two phenol molecules must bind to the site of action, and it is reassuring that the calculated energy change is neither impossibly large nor ludicrously small.

The position of the bound blocked state shown in Fig. 6A implies that phenol has an action equivalent to classical open channel block and that there are two separate sites of action. An alternative is to have the bound blocked state coming off the conducting bound open state, which implies a single site of action with a drug-bound transition between two states. Each position mimics the main experimental findings, but they are not kinetically equivalent. Our reasons for choosing the open channel block position relate to experiments on the effects of local anesthetics and *n*-alkanols performed in collaboration with J. P. Newman and J. A. Harrold (University of Dundee, Dundee, Scotland). Lidocaine and bupivacaine cause open-channel block-like increases in the tail decay time constant. We do not know the interaction between phenol and lidocaine in RCK1 channels, but Zamponi and French (8) suggest that for Na^+ channels, phenol mimics one of lidocaine's blocking modes. Our model is generally compatible with that suggestion; one of phenol's actions mimics the main effect of lidocaine (open channel block). The effects of *n*-

TABLE 2

Physical properties of phenol, *p*-cresol, and benzyl alcohol (from ref. 10)

Both phenols are better hydrogen bond donors (0.60 and 0.57) than acceptors (0.30 and 0.31) whereas benzyl alcohol is a better acceptor (0.56) than donor (0.33).

Compound	R_2	π_2^H	$\Sigma\alpha_2^H$	$\Sigma\beta_2^H$	V_x	P_{oct}	P_{hex}
Phenol	0.805	0.89	0.60	0.30	0.775	28.8	0.08
p-Cresol	0.820	0.87	0.57	0.31	0.916	93.3	0.65
Benzyl alcohol	0.803	0.87	0.33	0.56	0.916	12.6	0.37

R_2, excess molar refraction; π^H_2, dipolarity/polarizability of the molecule; $\Sigma\alpha^H_2$ summated hydrogen bond acidity (donor ability); $\Sigma\beta^H_2$ summated hydrogen bond basicity (acceptor ability); V_x, a volume term; P_{oct}, the octanol-water partition coefficient; P_{hex}, the hexadecane-water partition coefficient.

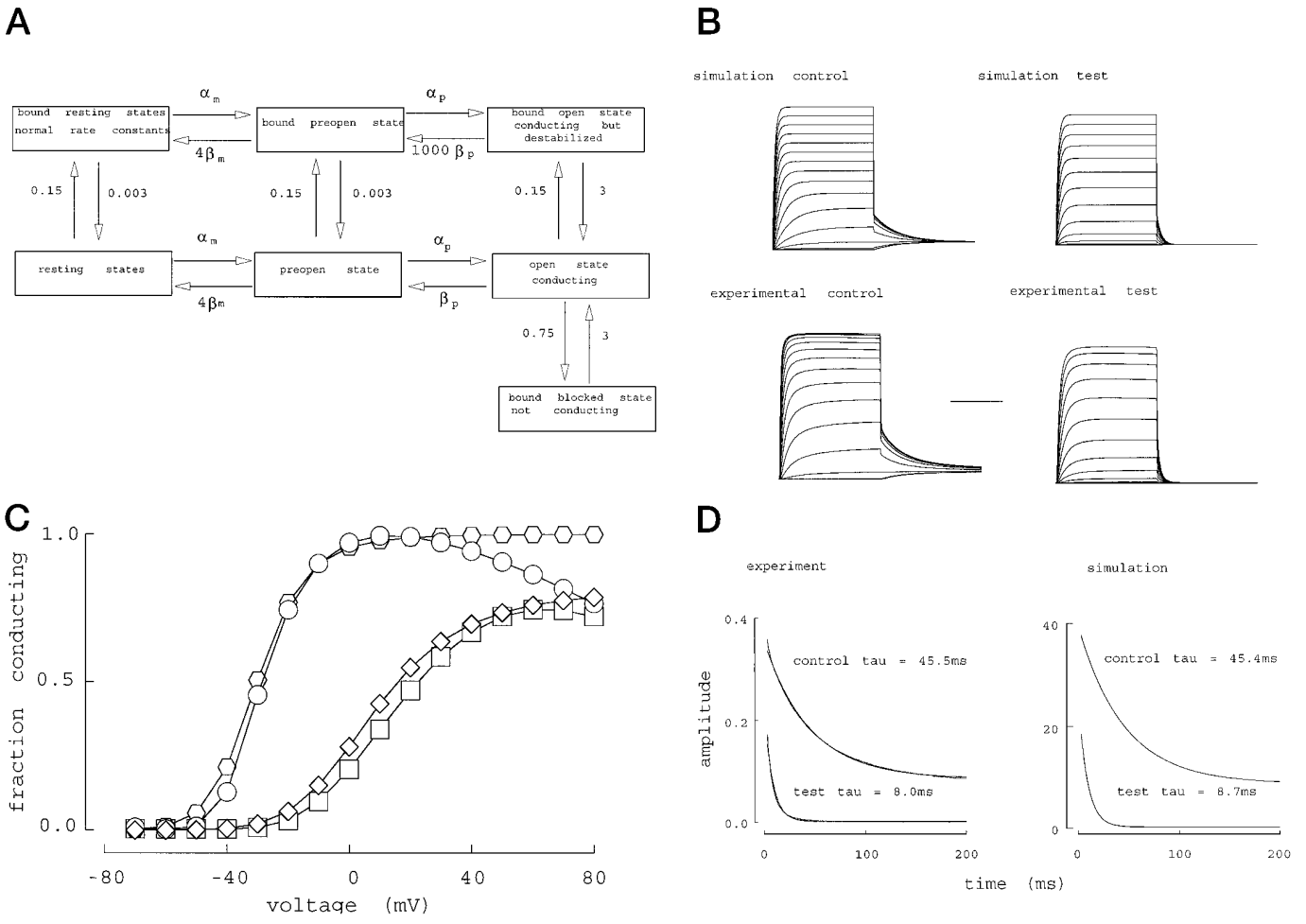

Fig. 6. Phenol and the RCK1 channel—a simple model. A, The control channel is modeled by a linear series of four resting states, a pre-open state, and an open state. The resting states (shown as one group) are linked by the standard 4:3:2:1 arrangement of α_m [0.5754 × exp(*V*/48)] and β_m [0.1691 × exp(−*V*/48)] rate constants (see, e.g., 29). The preopen and open states are linked by the rate constants α_p [0.24 × exp(0.0001 × *V*/24.56)] and β_p [0.004 × exp(−0.999 × *V*/24.56)]. *V,* simulation voltage. The depolarizing activation shift and accelerated tail kinetics were simulated by adding a parallel set of bound states in which the bound open state still conducts but is destabilized by a 1000-fold increase in β_p. This is matched by a 1000-fold increase in the binding affinity of resting and preopen states. A bound blocked state is included to account for current reduction additional to that induced by a depolarizing activation shift. The numbers indicate rate constants for binding or unbinding. B, A comparison of simulated and experimental currents. The experimental currents are averaged normalized data from four 2.5-mM phenol experiments. *Scale bar,* 100 msec. C, Fraction conducting versus voltage curves for (○) experimental control, (⎔) simulation control, (□) experimental test, and (◇) simulation test. D, Tail kinetics. Single exponential fits are shown superimposed on experimental and simulated tails.

pentanol on RCK1 channels can be explained by a mechanism very similar to the phenol model. *n*-Nonanol, however, has a much more obvious open-channel block behavior. Therefore, our model is formulated to produce a range of activity with classical open-channel block behavior at one end of the spectrum.

Concluding remarks. We have shown that phenol, at concentrations that have been measured in human serum after clinical administration, causes very large depolarizing shifts in the voltage dependence of RCK1 channel activation and a substantial acceleration of channel deactivation. The magnitude of these changes and the relative potencies of benzyl alcohol and *p*-cresol suggest a specific interaction with the channel itself, perhaps involving a strong hydrogen bond between the phenolic hydroxyl and an acceptor group on the channel protein. The depolarizing shift in activation threshold and the marked increase in deactivation kinetics are suggestive of a mechanism in which 1) phenol binding destabilizes but does not necessarily block open channels and 2) both resting and pre-open channels have a higher affinity for phenol than the open channel.

References

1. Morrison, J. E., Jr., D. Matthews, R. Washington, P. V. Fennessey, and M. Harrison. Phenol motor point blocks in children: plasma concentrations and cardiac dysrhythmias. *Anesthesiology* **75:**359–362 (1991).
2. Warner, M. A., and J. V. Harper. Cardiac dysrhythmias associated with chemical peeling with phenol. *Anesthesiology* **62:**366–367 (1985).
3. Gross, B. G. Cardiac arrhythmias during phenol face peeling. *Plast. Reconstr. Surg.* **73:**590–594 (1984).
4. Forrest, T., and D. T. O. Ramage. Cardiac dysrhythmia after subtrigonal phenol. *Anaesthesia* **42:**777–778 (1987).
5. Angel, A., and K. J. Rodgers. An analysis of the convulsant activity of substituted benzenes in the mouse. *Toxicol. Appl. Pharmacol.* **21:**214–229 (1972).
6. Otsuka, M., and Y. Nonomura. The action of phenolic substances on motor nerve endings. *J. Pharmacol. Exp. Ther.* **140:**41–45 (1962).
7. Kaila, K., and J. Saarikoski. Inhibition of voltage-dependent potassium conductance by convulsant phenols in the medial giant axon of the crayfish. *Comp. Biochem. Physiol.* **63C:**17–24 (1980).
8. Zamponi, G. W., and R. J. French. Dissecting lidocaine action: diethylam-

ide and phenol mimic separate modes of lidocaine block of sodium channels from heart and skeletal muscle. *Biophys. J.* **65:**2335–2347 (1993).
9. Stühmer, W., M. Stocker, B. Sakmann, P. Seeburg, A. Baumann, A. Grupe, and O. Pongs. Potassium channels expressed from rat brain cDNA have delayed rectifier properties. *FEBS Lett.* **242:**199–206 (1988).
10. Abraham, M. H., H. S. Chadha, G. S. Whiting, and R. C. Mitchell. Hydrogen bonding. 32. An analysis of water-octanol and water-alkane partitioning and the Δlog *P* parameter of Seiler. *J. Pharm. Sci.* **83:**1085–1100 (1994).
11. Elliott, A. A., and J. R. Elliott. Phenol inhibition of rat brain RCK1 (Kv1.1) K^+ channels expressed in *Xenopus* oocytes: implications for action potential firing in excitable cells. *J. Physiol. (Lond.)* **493:**81–82 (1996).
12. Constantinides, A. *Applied Numerical Methods with Personal Computers*. McGraw-Hill, New York (1987).
13. Ludewig, U., C. Lorra, O. Pongs, and S. H. Heinemann. A site accessible to extracellular TEA^+ and K^+ influences intracellular Mg^{2+} block of cloned potassium channels. *Eur. Biophys. J.* **22:**237–247 (1993).
14. Seeman, P. The membrane actions of anesthetics and tranquilizers. *Pharmacol. Rev.* **24:**583–655 (1972).
15. Nathan, P. W., and T. A. Sears. Effects of phenol on nervous conduction. *J. Physiol. (Lond.)* **150:**565–580 (1960).
16. Blaber, L. C., and J. P. Gallagher. The facilitatory effects of catechol and phenol at the neuromuscular junction of the cat. *Neuropharmacology* **10:**153–159 (1971).
17. Harrold, J. A., J. R. Elliott, and A. A. Elliott. Inhibition of oocyte-expressed rat brain IIa Na^+ channels by phenol. *p*-cresol and *n*-pentanol. *J. Physiol. (Lond.)* **497:**127P (1996).
18. Reyes, J., and R. Latorre. Effect of the anesthetics benzyl alcohol and chloroform on bilayers made from monolayers. *Biophys. J.* **28:**259–280 (1979).
19. Elliott, J. R., D. A. Haydon, and B. M. Hendry. The asymmetrical effects of some ionized *n*-octyl derivatives on the sodium current of the giant axon of *Loligo forbesi*. *J. Physiol. (Lond.)* **350:**429–445 (1984).
20. Strichartz, G. R., G. S. Oxford, and F. Ramon. Effects of the dipolar form of phloretin on potassium conductance in squid giant axons. *Biophys. J.* **31:**229–246 (1980).
21. Andersen, O. S., A. Finkelstein, I. Katz, and A. Cass. Effect of phloretin on the permeability of thin lipid membranes. *J. Gen. Physiol.* **67:**749–771 (1976).
22. Klusemann, J., and H. Meves. Phloretin affects the fast potassium channels in frog nerve fibres. *Eur. Biophys. J.* **20:**79–86 (1991).
23. Lide, D. R., and H. P. R. Frederikse. *CRC Handbook of Chemistry and Physics*. CRC Press, Boca Raton, FL (1995).
24. Kitagawa, S., and H. Hirata. Effects of alcohols on fluorescence anisotropies of diphenylhexatriene and its derivatives in bovine blood platelets: relationships of the depth-dependent change in membrane fluidity by alcohols and their effects on platelet aggregation and adenylate cyclase activity. *Biochim. Biophys. Acta* **1112:**14–18 (1992).
25. Kitagawa, S., M. Orinaka, and H. Hirata. Depth-dependent change in membrane fluidity by phenolic compounds in bovine platelets and its relationship with their effects on aggregation and adenylate cyclase activity. *Biochim. Biophys. Acta* **1179:**277–282 (1993).
26. Abraham, M. H., W. R. Lieb, and N. P. Franks. Role of hydrogen bonding in general anesthesia. *J. Pharm. Sci.* **80:**719–724 (1991).
27. Urban, B. W., and D. A. Haydon. The actions of halogenated ethers on the ionic currents of the squid giant axon. *Proc. R. Soc. Lond. B Biol. Sci.* **231:**13–26 (1987).
28. Harper, A. A., A. G. Macdonald, and K. T. Wann. The effect of temperature on the nerve-blocking action of benzyl alcohol on the squid giant axon. *J. Physiol. (Lond.)* **338:**51–60 (1983).
29. Koren, G., E. R. Liman, D. E. Logothetis, B. Nadal-Ginard, and P. Hess. Gating mechanism of a cloned potassium channel expressed in frog oocytes and mammalian cells. *Neuron* **2:**39–51 (1990).
30. Hille, B. *Ionic Channels of Excitable Membranes*. 2nd ed. Sinauer Associates Inc., Sunderland, MA (1992).
31. Jeffrey, G. A., and W. Sanger. *Hydrogen bonding in biological structures.* Springer-Verlag, Berlin (1994).
32. Schneider, H.-J., T. Blatter, S. Simonova, and I. Theis. Large binding constant differences between aromatic and aliphatic substrates in positively charged cavities indicative of higher order electrical effects. *J. Chem. Soc. Chem. Comm.* **9:**580–581 (1989).

Send reprint requests to: Dr. J.R. Elliott, Department of Anatomy and Physiology, University of Dundee, Dundee DD1 4HN, United Kingdom. E-mail: j.r.elliott@dundee.ac.uk